

Received September 2, 2016, accepted September 14, 2016, date of publication October 19, 2016,
date of current version November 28, 2016.

Digital Object Identifier 10.1109/ACCESS.2016.2618373

On the Robust Trajectory Tracking Task for Flexible-Joint Robotic Arm With Unmodeled Dynamics

**MARIO RAMÍREZ-NERIA¹, GILBERTO OCHOA-ORTEGA², NORMA LOZADA-CASTILLO³,
MIGUEL ANGEL TRUJANO-CABRERA², JUAN PABLO CAMPOS-LÓPEZ²,
AND ALBERTO LUVIANO-JUÁREZ⁴**

¹Automatic Control Department, CINVESTAV-IPN, 07360 Mexico City, Mexico

²Division of Mechatronics, Mexico's Valley Polytechnic University, Polytechnic, 54910 Tultitlan, Mexico

³National Polytechnic Institute-ESIME Zacatenco, Zacatenco , 07738 Mexico City, Mexico

⁴National Polytechnic Institute-UPIITA, UPIITA, 07340 Mexico City, Mexico

Corresponding author: G. Ochoa-Ortega (gochoa79@gmail.com)

ABSTRACT This paper is concerned with the design and experimental assessment of, both, feedback linearization and sliding mode control techniques to the tracking trajectory problem of a flexible-joint robotic arm for a smooth rest to rest maneuver. The robust improvement of these controllers is analyzed by means of additional integral compensation, in which an alternative sliding surface was proposed for the control of the flexible arm. A feedback linearization of the nonlinear dynamic equation of the robot arm is computed in order to get a full-state non-linear feedback control law. On the other hand, it is proposed a second order sliding mode control with an integral term in the sliding surface, which improves the robustness of the controller sliding surface. Some experimental evaluations that include the addition of external unmodeled perturbations to test the enhancement of the robustness property show the improvements and effectiveness of the proposed control laws in disturbance rejection tasks. The controllers were implemented using exclusively position measurements and time derivatives approximations.

INDEX TERMS Feedback linearization, sliding mode control, robustness, flexible-joint robotic systems.

I. INTRODUCTION

The control of flexible manipulators has been studied with great interest by, both, practical engineers as well as academic researchers. This is mainly because the application of control algorithms for rigid joint robotic manipulators is limited, and their direct application may lead to poor results. The nature of flexible joint systems is generated by pulleys, timing belts or harmonic drives causing a flexible joint phenomenon. On the other hand, the flexible link model effect can be arisen by increasing payload-to-weight ratio, motion speed or control bandwidth, see [34]. In both cases, this class of systems increases its order, as well as, the difficulties to control its end-position.

Some natural benefits of flexible joints include:

- Arising of mechanical impedance [44]. This aspect is helpful in human robot interaction tasks [42]. Also it provides protection of the mechanisms against impacts and torque reduction in the actuators.
- The flexibility allows a mechanical energy storage, which is helpful in a wide class of applications

(orthosis, prosthetic devices, flexible manipulators, etc) and semi active systems (structural damping systems, among others) [12], [19].

Some control approaches have been proposed for the stabilization and trajectory tracking control of flexible joints. For instance, robust control schemes [10], [14], [16], [18], [24], [30], adaptive control [9], [21], [35], backstepping [3], passivity based control [33], recursive methods [45], extended state observers [37], saturated control [4], among others. All these control schemes are based on nonlinear control strategies that can be applied to highly nonlinear dynamic systems. These nonlinear approaches may not provide robustness for controlling flexible robotic manipulators, mainly since most of them require the complete knowledge of the mathematical model or, at least, an approximate one. To overcome this restriction, fuzzy controllers [11], [22], [38] have been developed because its structure is rather simple in comparison with other model-based controllers. However, fuzzy control usually takes up a considerable computation time, the gain tuning may be exhausting, and it needs to be

simplified [13]. In other cases, hybrid control laws have been developed considering the combination of fuzzy and H_∞ control [28], fuzzy logic and discontinuous control techniques [23], fuzzy logic and neural networks [36], in order to reject oscillations and achieve a good tracking performance.

Generally, a flexible-joint robot cannot be linearized by static feedback [39]. However, an alternative simplified model was provided that, under some assumptions, it can be feedback linearizable [34]. In [8], it was proven that the whole class of elastic joint robots can be linearized via dynamic feedback. In [7], [27], [29], some feedback linearization controllers are presented.

On the other hand, the sliding mode control method [40], can compensate uncertainties in the dynamic parameters of the robot arm as well as disturbance inputs. The basic idea behind the sliding mode control is to apply a discontinuous feedback control law in order to drive the system, in a finite time, to a desire surface, called *sliding surface*, in the state space. Some examples of sliding mode controllers in flexible joint arms are found in [6], [17], [26], [43] and the references therein. In general, the sliding surface depends on the phase state of the system achieving good results. However, an appropriate sliding surface extending the phase state of the system using integral terms can improve the robustness response of the closed loop system in practical applications which are prone to be subject to disturbance inputs. This idea has been comprehensively developed in classic control schemes such as PD/PID, with a less specialized theoretical knowledge and taken in alternative control schemes where integral compensation terms have been used to reject a wider class of disturbance inputs [46].

In this contribution the tracking problem of a Flexible-Joint Robotic Arm for a smooth rest to rest maneuver avoiding undesirable oscillations is addressed by means of two control approaches with additional integral terms, one for a classic feedback linearization and another one in the case of the surface of a high order sliding mode controller. To design the control law via feedback linearization, it is followed the scheme presented in [15] based on an appropriate coordinate transformation to turn the given dynamics into a linear and controllable system. In this case, in contrast with most of the existing works, the output function is given in terms of the addition of two angular positions. In the case of the sliding mode control, it is defined a variation of the sliding surface in the Super Twisting control approach, by adding an integral term (see [41]) which guarantees a stabilizing sliding mode control, while increasing the robustness with respect to the nonlinearities in the state space description as well as external disturbance inputs.

The manuscript is organized as follows: Section II the dynamic model of the flexible joint robot arm under study and the problem formulation are presented. The design of the proposed non-linear control laws is developed in Section III. Section IV shows the experimental results of the proposed control laws. A classical PID, is taken as a starting point for the controllers analysis behavior and the same schemes

without the integral compensation are included to show the improvement of the presented proposal. Concluding remarks end this contribution.

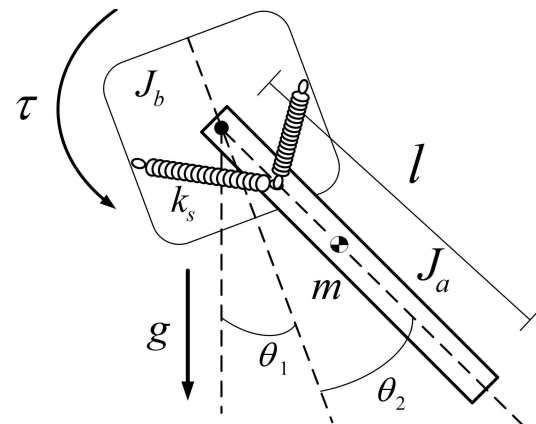


FIGURE 1. Schematic of Flexible-Joint Robot Arm.

II. FLEXIBLE JOINT ROBOT DYNAMICS

In this contribution a single Flexible Joint Robotic system, as shown in Figure 1, is analyzed. The following parameters and variables are considered

- θ_1 Angular position of the rotating base
- θ_2 Angular position of the arm
- J_a Moment of inertia of the arm
- J_b Moment of inertia of the rotating base
- m Mass of the arm
- l Arm length
- k_s Spring stiffness
- τ Torque applied to the system

The angular position of the arm tip is defined by the relation

$$\vartheta = \theta_1 + \theta_2$$

In order to determine the dynamic model of the flexible-joint robot, the Euler-Lagrange approach was followed. The Lagrangian of the system is

$$\mathcal{L} = K - V$$

where K represents the kinetic energy and V the potential energy.

The kinetic energy of the system is given by

$$K = K_b + K_a$$

where K_b represents the kinetic energy of the rotating base, and K_a represents the kinetic energy of the arm.

The potential energy of the system satisfies the relation

$$V = V_s + V_a$$

where V_s is the potential energy associated to the spring, and V_a is the potential energy associated with the arm.

Thus, the Lagrangian of the system is given by

$$\mathcal{L} = \frac{J_b}{2}\dot{\theta}_1^2 - \frac{k_s}{2}\theta_2^2 + \frac{J_a}{2}\dot{\vartheta}^2 + \frac{mgl}{2}\cos(\vartheta)$$

Applying the Euler Lagrange equation for the generalized coordinates θ_1, θ_2 , lead us to the equations

$$\begin{aligned}\tau &= J_b\ddot{\theta}_1 + J_a\ddot{\vartheta} + \frac{mgl}{2}\sin(\vartheta) \\ 0 &= J_a\ddot{\vartheta} + K_s\theta_2 + \frac{mgl}{2}\sin(\vartheta)\end{aligned}$$

Now, on the one hand, the motor torque τ_m and the torque applied to the system are related as: $\tau = N\tau_m$, N represents the mechanical advantage of the pulley system. On the other hand, the voltage applied to the motor, and the torque generated by it, satisfies the relation

$$\tau_m = \frac{k_\tau}{R_m}V(t) - \frac{k_\tau^2 N^2}{R_m}\dot{\theta}_1$$

where R_m denotes the armature resistance, k_τ represents the torque constant of the motor and the control input of the system is denoted by $V(t)$. With this last relation, the dynamics of the flexible-joint robot, are given by

$$\begin{aligned}\frac{Nk_\tau}{R_m}V(t) &= (J_b + J_a)\ddot{\theta}_1 + J_a\ddot{\vartheta}_2 + \frac{k_\tau^2 N^2}{R_m}\dot{\theta}_1 \\ &\quad + \frac{mgl}{2}\sin(\vartheta)\end{aligned}\quad (1)$$

$$0 = J_a\ddot{\vartheta} + K_s\theta_2 + \frac{mgl}{2}\sin(\vartheta) \quad (2)$$

and $\ddot{\theta}_1$ and $\ddot{\theta}_2$ can be fully determined as follows

$$\ddot{\theta}_1 = \frac{k_s}{J_b}\theta_2 - \frac{k_\tau^2 N^2}{J_b R_m}\dot{\theta}_1 + \frac{k_\tau N}{J_b R_m}V(t) \quad (3)$$

$$\begin{aligned}\ddot{\theta}_2 &= -\frac{k_s(J_a + J_b)}{J_a J_b}\theta_2 - \frac{mgl}{2J_a}\sin(\theta_1 + \theta_2) \\ &\quad + \frac{k_\tau^2 N^2}{J_b R_m}\dot{\theta}_1 - \frac{k_\tau N}{J_b R_m}V(t)\end{aligned}\quad (4)$$

A. PROBLEM FORMULATION

It is desired to move the main arm end-point from an initial rest angular position $y(0) = \theta_1(0) + \theta_2(0)$ to a final rest angular position, $y(T)$, within the time interval $[0, T]$, while following a pre-specified trajectory $y^*(t)$ defined as a smooth rest to rest maneuver, by means of interpolation of Bézier type polynomials. It is desirable that the angular position of the link tip arrives to its final destination without oscillations in spite of disturbances, non modelled nonlinearities or external perturbations.

III. NONLINEAR CONTROL DESIGN

If we define the state variables

$$\begin{aligned}x_1 &= \theta_1 & x_3 &= \theta_2 \\ x_2 &= \dot{\theta}_1 & x_4 &= \dot{\theta}_2\end{aligned}$$

system (3)-(4), can be rewritten in the state space representation as:

$$\dot{x} = f(x) + gV(t) \quad (5)$$

where

$$f(x) = \begin{bmatrix} x_2 \\ \frac{k_s}{J_b}x_3 - \frac{k_\tau^2 N^2}{J_b R_m}x_2 \\ x_4 \\ \frac{k_\tau^2 N^2}{J_n R_m}x_2 - \frac{k_s(J_a + J_b)}{J_a J_b}x_3 - \frac{mgl}{2J_a}\sin(x_1 + x_3) \end{bmatrix}$$

and

$$g = \begin{bmatrix} 0 & \frac{k_\tau N}{J_b R_m} & 0 & -\frac{k_\tau N}{J_b R_m} \end{bmatrix}^\top$$

A. ROBUST FEEDBACK LINEARIZATION CONTROLLER

To determine the control law via feedback linearization, we follow the scheme presented in [15]. In this case, the following output function is proposed

$$h(x) = x_1 + x_3$$

The first step in this strategy, is to determine the relative degree of the system, and in order to determine it, we must first compute the derivative of the output function, defined as

$$\dot{h}(x) = \frac{\partial h(x)}{\partial x}\dot{x} = L_f h(x) + L_g h(x)$$

where $L_f h(x)$ and $L_g h(x)$ denote the Lie derivative of the output function $h(x)$, with respect to $f(x)$ and $g(x)$ respectively. Then

$$L_f h(x) = x_2 + x_4$$

$$L_g h(x) = 0$$

therefore, the higher order time derivatives are expressed as

$$\ddot{h}(x) = L_f^2 h(x) + V(t)L_g L_f h(x)$$

$$h^{(3)}(x) = L_f^3 h(x) + V(t)L_g L_f^2 h(x)$$

$$h^{(4)}(x) = L_f^4 h(x) + V(t)L_g L_f^3 h(x)$$

where

$$L_f^2 h(x) = \gamma x_3 - \alpha_4 \sin(x_1 + x_3)$$

$$L_g L_f h(x) = 0$$

$$L_f^3 h(x) = -\alpha_4(x_2 + x_4)\cos(x_1 + x_3) + \gamma x_4$$

$$L_g L_f^2 h(x) = 0$$

$$\begin{aligned}L_f^4 h(x) &= \alpha_4 \sin(x_1 + x_3) \left[(x_2 + x_4)^2 - \gamma \right. \\ &\quad \left. + \alpha_4 \cos(x_1 + x_3) \right] + \gamma(\alpha_1 x_2 - \alpha_3 x_3) \\ &\quad + \alpha_4 x_3 \cos(x_1 + x_3)(\alpha_3 - \alpha_2)\end{aligned}$$

$$L_g L_f^3 h(x) = -\gamma \beta$$

Since $L_g L_f^3 h(x) \neq 0$ in the whole state space, the relative degree of the system (with respect to the output function $h(x)$) is four.

By defining the following change of coordinates

$$\begin{aligned} z_1 &= h(x) & z_2 &= \dot{h}(x) & z_3 &= \ddot{h}(x) \\ z_4 &= h^{(3)}(x) & z_5 &= h^{(4)}(x) \end{aligned}$$

system (5), in the new coordinates representation, appears as

$$\begin{aligned} \dot{z}_1 &= L_f h(x) \\ \dot{z}_2 &= L_f^2 h(x) \\ \dot{z}_3 &= L_f^3 h(x) \\ \dot{z}_4 &= L_f^4 h(x) + V(t) L_g L_f h(x) \end{aligned} \quad (6)$$

The desired trajectory and its time derivatives are denoted as $h^*(x) = z_1^*$ and $h^{(i)*}(x) = z_{(i+1)}^*$, $i = 1, 2, 3, 4$, respectively. This definition allow us expressing the tracking trajectory error as, $e z_i = z_i - z_i^*$, and a linearizing control input function $V(t)$ can be proposed as follows

$$V(t) = \frac{1}{L_g L_f^3 h(x)} [\tilde{u}(t) - L_f^4 h(x)] \quad (7)$$

Therefore, system (6), can be rewritten in terms of the tracking trajectory error, as a linear system of the form

$$\begin{aligned} \dot{e}z_1 &= e z_2 \\ \dot{e}z_2 &= e z_3 \\ \dot{e}z_3 &= e z_4 \\ \dot{e}z_4 &= \tilde{u}(t) \end{aligned} \quad (8)$$

The above system represents an integrator chain of fourth order, that can be stabilized by means of the following auxiliary controller

$$\tilde{u}(t) = -k_1 e z_1 - k_2 e z_2 - k_3 e z_3 - k_4 e z_4 + z_5^*$$

The control gains k_i , $i = 1, \dots, 4$ are chosen, in such a way, that the closed-loop poles of the linearized system match with the dynamics of a proposed stable characteristic polynomial

$$\begin{aligned} p(s)_{FL} &= (s^2 + 2\xi_{FL}\omega_{FL}s + \omega_{FL}^2)^2 \\ &= s^4 + k_4 s^3 + k_3 s^2 + k_2 s + k_1 \end{aligned}$$

Here $\xi_{FL}, \omega_{FL} \in \mathbb{R}^+$.

The parameters k_i , $i = 1, 2, 3, 4$, of the auxiliary controller $\tilde{u}(t)$, are assigned as follows

$$\begin{aligned} k_1 &= \omega_{FL}^4 \\ k_2 &= 4\xi_{FL}\omega_{FL}^3 \\ k_3 &= 2\xi_{FL}^2 + 4\xi_{FL}\omega_{FL}^2 \\ k_4 &= 4\xi_{FL}\omega_{FL} \end{aligned} \quad (9)$$

To improve the robustness property of the system in the presence of parametric variations, small parametric uncertainties in the model dynamics or external shocks, a compensator in the classic structural sense will be implemented, where one of the most popular and used is an integral compensation.

For the linear system (8), the auxiliary control is established as follows

$$\begin{aligned} \tilde{u}(t) &= -\lambda_0 \int_0^t e(\epsilon) z_1 d\epsilon - \lambda_1 e z_1 - \lambda_2 e z_2 - \lambda_3 e z_3 \\ &\quad - \lambda_4 e z_4 + z_5^* \end{aligned}$$

As in the previous section, gains $\lambda_0, \dots, \lambda_4$ are chosen, according the dynamics of the following auxiliary polynomial

$$\begin{aligned} p(s)_{IFL} &= (s + p_{IFL}) (s^2 + 2s\xi_{IFL}\omega_{IFL} + \omega_{IFL}^2)^2 \\ &= s^5 + \lambda_4 s^4 + \lambda_3 s^3 + \lambda_2 s^2 + \lambda_1 s + \lambda_0 \end{aligned}$$

that is:

$$\begin{aligned} \lambda_0 &= p_{IFL}\omega_{IFL}^4 \\ \lambda_1 &= \omega_{IFL}^4 + 4p_{IFL}\xi_{IFL}\omega_{IFL}^3 \\ \lambda_2 &= 4\xi_{IFL}\omega_{IFL}^3 + 4p_{IFL}\xi_{IFL}^2\omega_{IFL}^2 \\ &\quad + 2p_{IFL}\omega_{IFL}^2 \\ \lambda_3 &= 4\xi_{IFL}^2\omega_{IFL}^2 + 2\omega_{IFL}^2 + 4p_{IFL}\xi_{IFL}\omega_{IFL} \\ \lambda_4 &= 4\xi_{IFL}\omega_{IFL} + p_{IFL} \end{aligned} \quad (10)$$

Here $\xi_{IFL}\omega_{IFL} \in \mathbb{R}^+$

B. ROBUST SUPER-TWISTING SLIDING MODE CONTROL

The classical first order sliding mode control methodology is a discontinuous robust feedback technique, whose main disadvantage, is the appearance of chattering [5], [31], which may rise due to neglected fast dynamics or to digital implementation issues [40]. This phenomenon is characterized by high frequency oscillations at the output system that can be harmful when the controller is applied in motion control systems. In order to reduce this phenomenon and reject perturbations, a higher order sliding mode control is proposed [1], [20]. First of all, the following sliding manifold is proposed

$$\begin{aligned} \sigma(t) &= (z_4 - z_5^*) + \alpha_3(z_3 - z_3^*) + \alpha_2(z_2 - z_2^*) \\ &\quad + \alpha_1(z_1 - z_1^*) \end{aligned}$$

where the parameters α_1 , α_2 , and α_3 must be selected, in such a way, that ensures the ideal conditions $\sigma = 0$ and $\dot{\sigma} = 0$ are satisfied. From the derivative condition we obtain

$$\begin{aligned} 0 &= (z_5 - z_5^*) + \alpha_3(z_4 - z_4^*) + \alpha_2(z_3 - z_3^*) \\ &\quad + \alpha_1(z_2 - z_2^*) \end{aligned}$$

To guarantee the convergence of the states to the desired trajectory (under the validity of ideal condition $\sigma = 0$), that is, $z_1 \rightarrow z_1^*$, $z_2 \rightarrow z_2^*$, $z_3 \rightarrow z_3^*$, and $z_4 \rightarrow z_4^*$, the parameters α_i , $i = 1, 2, 3$ are selected following the dynamics of proposed Hurwitz polynomial

$$\begin{aligned} p(s)_{SM} &= (s^2 + 2\xi_{SM}\omega_{SM}s + \omega_{SM}^2)(s + p_{SM}) \\ &= s^3 + \alpha_3 s^2 + \alpha_2 s + \alpha_1 \end{aligned}$$

where $\xi_{SM}, \omega_{SM} \in \mathbb{R}^+$, that is

$$\begin{aligned} \alpha_1 &= p_{SM}\omega_{SM}^2 \\ \alpha_2 &= \omega_{SM}^2 + 2p_{SM}\xi_{SM}\omega_{SM} \\ \alpha_3 &= p_{SM} + 2\xi_{SM}\omega_{SM} \end{aligned} \quad (11)$$

Now, the time derivative of the sliding manifold is of the form

$$\dot{\sigma}(t) = (z_5 - z_5^*) + \alpha_3(z_4 - z_4^*) + \alpha_2(z_3 - z_3^*) + \alpha_1(z_2 - z_2^*)$$

Substituting (6), the previous expression takes the form

$$\begin{aligned}\dot{\sigma}(t) &= V(t)L_g L_f^3 h(x) + L_f^4 h(x) - z_5^* + \alpha_3(z_4 - z_4^*) \\ &\quad + \alpha_2(z_3 - z_3^*) + \alpha_1(z_2 - z_2^*)\end{aligned}\quad (12)$$

we define $\eta(t)$ as a lumped bounded disturbance function

$$\begin{aligned}\eta(t) &= L_f^4 h(x) - z_5^* + \alpha_3(z_4 - z_4^*) + \alpha_2(z_3 - z_3^*) \\ &\quad + \alpha_1(z_2 - z_2^*) + \Psi(t)\end{aligned}$$

where $\Psi(t)$ is the bounded external unknown disturbance, equation (12) can be determinated as

$$\dot{\sigma}(t) = V(t)L_g L_f^3 h(x) + \eta(t)$$

The Super Twisting sliding mode control is proposed as follows

$$\begin{aligned}V(t) &= \frac{1}{L_g L_f^3 h(x)}(-a\sqrt{|\sigma(t)|}\text{sign}(\sigma(t)) + y) \\ \dot{y} &= -W\text{sign}(\sigma(t))\end{aligned}\quad (13)$$

In order to increase the robustness of Super-Twisting controller, it is proposed the following sliding manifold including an integral term [2], [41].

$$\begin{aligned}\sigma(t) &= (z_4 - z_4^*) + \alpha_3(z_3 - z_3^*) + \alpha_2(z_2 - z_2^*) \\ &\quad + \alpha_1(z_1 - z_1^*) + \alpha_0 \int_0^t (z_1(\gamma) - z_1(\gamma)^*) d\gamma\end{aligned}\quad (14)$$

where the parameters α_0 , α_1 , α_2 and α_3 must be selected, in such a way, that ensures the ideal conditions $\sigma = 0$ and $\dot{\sigma} = 0$.

$$\begin{aligned}p(s)_{ISM} &= (s^2 + 2\xi_{ISM}\omega_{ISM}s + \omega_{ISM}^2)^2 \\ &= s^4 + \alpha_3 s^3 + \alpha_2 s^2 + \alpha_1 s + \alpha_0\end{aligned}$$

where $\xi_{ISM}, \omega_{ISM} \in \mathbb{R}^+$, that is

$$\begin{aligned}\alpha_0 &= \omega_{ISM}^4 \\ \alpha_1 &= 4\xi_{ISM}\omega_{ISM}^3 \\ \alpha_2 &= 2\xi_{ISM}^2 + 4\xi_{ISM}^2\omega_{ISM}^2 \\ \alpha_3 &= 4\xi_{ISM}\omega_{ISM}\end{aligned}\quad (15)$$

In the following theorem, conditions of finite time convergence are provided. This property is crucial for high-precision performance on control systems of engineering applications.

Proposition 1: Given a sliding manifold of the form (14), then if conditions

$$\kappa_1 > \frac{2\delta\kappa_2}{\kappa_2 - 1}, \quad \kappa_2 > 1, \quad \kappa_3 = \frac{\kappa_2 - 1}{2\delta}$$

are satisfied, then the zero conditions ($\sigma(t) = \dot{\sigma}(t) = 0$) are satisfied in finite time $T = \frac{2\lambda_{max}(P)}{\sqrt{\lambda_{min}(P)}} V^{\frac{1}{2}}(t) \xi(0)$ setting the gain controller as

$$\begin{aligned}W &= \frac{\kappa_1 + a\kappa_2}{\kappa_3} \\ a &= \frac{\kappa_2(\delta\kappa_3 - \kappa_1) - \kappa_3(1 - 2\delta\kappa_3)}{\kappa_2^2 - \kappa_1\kappa_3}\end{aligned}$$

Proof 2: The proof follows the methodology presented in [41] and [25]. Under the transformation

$$\xi(t) = \tilde{\eta}(t) - W \int_0^t \text{sign}(\sigma(\tau)) d\tau$$

where

$$\begin{aligned}\tilde{\eta}(t) &= L_f^4 h(x) - z_5^* + \alpha_3(z_4 - z_4^*) + \alpha_2(z_3 - z_3^*) \\ &\quad + \alpha_1(z_2 - z_2^*) + \alpha_0(z_1 - z_1^*) + \Psi(t)\end{aligned}$$

the time derivative of (14) can be expressed as

$$\begin{aligned}\dot{\sigma}(t) &= -a\sqrt{|\sigma(t)|}\text{sign}(\sigma(t)) + \xi(t) \\ \dot{\xi}(t) &= -W\text{sign}(\sigma(t)) + \dot{\tilde{\eta}}(t)\end{aligned}\quad (16)$$

Let us define $c = [\sqrt{|\sigma(t)|}\text{sign}(\sigma(t)), \xi(t)]^\top$, and the candidate Lyapunov function

$$V(t) = \frac{1}{2} c^\top P c, \quad P = \begin{bmatrix} \kappa_1 & -\kappa_2 \\ -\kappa_2 & \kappa_3 \end{bmatrix}$$

where $\kappa_{1,2,3} > 0$, satisfying $|P| > 0$ to guarantee the positiveness of $V(t)$. Then, the time derivative of the function $V(t)$ along the solutions of system (16) is given by

$$\begin{aligned}\frac{dV(t)}{dt} &= -\frac{1}{2|\sigma(t)|^{\frac{1}{2}}} c^\top Q_0 c \\ &\quad + \frac{\dot{\tilde{\eta}}(t)}{2} (\xi\kappa_3 - |\sigma(t)|^{\frac{1}{2}}\text{sign}(\sigma(t))\kappa_2)\end{aligned}\quad (17)$$

Here

$$Q_0 = \begin{bmatrix} a\kappa_1 - W\kappa_2 & -\frac{1}{2}(\kappa_1 + a\kappa_2 - W\kappa_3) \\ -\frac{1}{2}(\kappa_1 + a\kappa_2 - W\kappa_3) & \kappa_2 \end{bmatrix}$$

By direct computations, the last term of the right hand side of the equality, can be expressed as

$$-\frac{\dot{\tilde{\eta}}(t)}{2|\sigma(t)|^{\frac{1}{2}}} c^\top Q_1 c$$

where

$$Q_1 = \begin{bmatrix} \kappa_2 - 2\kappa_3 & 0 \\ 0 & -2\kappa_3 \end{bmatrix}$$

then, under the assumption that $|\dot{\tilde{\eta}}(t)| \leq \delta$, (17) takes the form

$$\frac{dV(t)}{dt} \leq -\frac{1}{2|\sigma(t)|^{\frac{1}{2}}} c^\top [Q_0 + \delta Q_1] c$$

Setting $Q_2 = Q_0 + \delta Q_1 = I_{2 \times 2}$, the following relations are satisfied

$$\kappa_1 > \frac{2\delta\kappa_2}{\kappa_2 - 1}, \quad \kappa_2 > 1, \quad \kappa_3 = \frac{\kappa_2 - 1}{2\delta}$$

and the controller gains are defined as

$$W = \frac{\kappa_1 + a\kappa_2}{\kappa_3} \quad (18)$$

$$a = \frac{\kappa_2(\delta\kappa_3 - \kappa_1) - \kappa_3(1 - 2\delta\kappa_3)}{\kappa_2^2 - \kappa_1\kappa_3} \quad (19)$$

From Rayleigh's inequality the following inequalities are satisfied

$$\frac{dV(t)}{dt} \leq -\frac{1}{2|\sigma(t)|^{\frac{1}{2}}\lambda_{max}(P)}\|c\|^2$$

$$\sqrt{\lambda_{min}(P)}|\sigma(t)|^{\frac{1}{2}} \leq V^{\frac{1}{2}}(t)$$

then

$$\frac{dV(t)}{dt} \leq -\frac{\sqrt{\lambda_{min}(P)}}{\lambda_{max}(P)}V^{\frac{1}{2}}(t)$$

then, it follows that the equilibrium point at the origin is reached in finite time smaller than

$$T = \frac{2\lambda_{max}(P)}{\sqrt{\lambda_{min}(P)}}V^{\frac{1}{2}}(t)\xi(0)$$

■

IV. PROTOTYPE ARCHITECTURE AND EXPERIMENTAL RESULTS

In this section the instrumentation and set up of the Flexible-Joint Robotic Arm prototype are presented. The designed control laws were, both, implemented in Matlab-Simulink through a Data Acquisition device. Some rest to rest tracking results by using a classic controller, as well as the proposed schemes are also presented to illustrate the effectiveness of the proposals.

A. IMPLEMENTATION OF THE CONTROLLER PLATFORM

Figure 2 shows the diagram of the experimental platform used to control the Flexible-Joint Robotic Arm system.

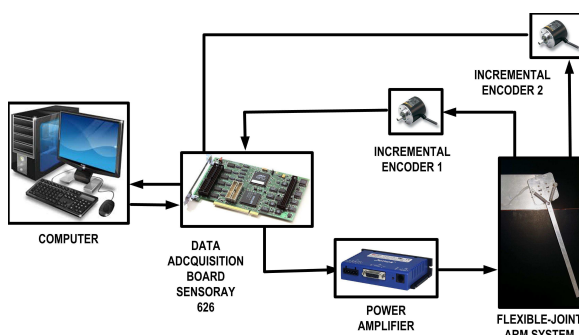


FIGURE 2. Block diagram for the Flexible-Joint Robotic Arm control scheme.

The experimental device is shown in Figure 3. It consists of a DC motor NISCA: model NC5475, which drives a rotating base through a synchronous belt and pulley system with a 16:1 ratio. The main arm is attached to the rotating base by two identical springs, resulting in a flexible joint. Both, the angular positions of the rotating base and the arm were measured with incremental optical encoders of 1000 pulses/revolution. The data acquisition is carried out through a data card Sensoray model 626. This board, is responsible to read the signals from the optical incremental encoders and supplies control voltages to the power amplifiers. The control strategies were implemented in the

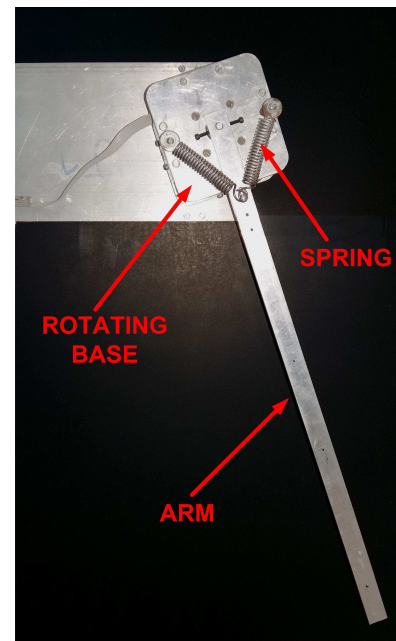


FIGURE 3. Flexible-Joint Robot Arm system prototype.

Matlab-Simulink environment, and the devised control signals were transferred to the actuators through three power amplifiers Sanyo, model STK4050II. Finally, the sampling time was set to be 0.001[s]. The Flexible-Joint Robot Arm parameters, used to implement the control laws are: $l = 0.5[\text{m}]$, $m = 0.1633[\text{Kg}]$, $J_a = 0.0136[\text{Kg}\cdot\text{m}^2]$, $J_b = 0.002405[\text{Kg}\cdot\text{m}^2]$, $k_s = 4[\text{N}\cdot\text{m}/\text{rad}]$ and $N = 16$, while the motor parameters are: $k_t = 0.0724[\text{N}\cdot\text{m}/\text{A}]$ and $R_m = 2.983 [\Omega]$.

B. EXPERIMENTAL RESULTS

1) TRACKING TRAJECTORY PROBLEM FORMULATION

The considered set of initial conditions for the system are: $[\theta_1(0) = 0, \theta_2(0) = 0]$. The desired trajectory that the Flexible-Joint Arm Robot must achieve is defined as follows: the path is initialized at $y^*(0) = 0[\text{rad}]$ at time $t = 0[\text{s}]$, then when $t = 2[\text{s}]$ the mechanism is moved, in an interval of $0.6[\text{s}]$, to $y^*(t) = \frac{\pi}{2}[\text{rad}]$, the trajectory remains in this position for $7.4[\text{s}]$. Finally, when time reach $10[\text{s}]$, the reference trajectory returns to $y^*(t) = 0[\text{rad}]$, in a interval of time $0.6[\text{s}]$, and the device stays in this position until the experiment ends. This trajectory takes 18 seconds to be completed and it will be used throughout the experimental tests.

2) PID CONTROLLER

In order to show the inevitably oscillations induced at the end-effector due to the flexibility of the manipulator. We propose a traditional PID controller for the position of the rotating base θ_1 regardless the position of the arm θ_2 , where the desired rest to rest trajectory for the rotating base position is specified as $\theta_1^*(t) = y^*(t)$. Here, the PID controller is of

the form

$$V_{PID}(t) = -k_P (\theta_1(t) - y^*(t)) - k_D (\dot{\theta}_1(t) - \dot{y}^*(t)) - k_I \int (\theta_1(t) - y^*(t)) dt$$

where the design parameters are specified as: $k_P = 40$, $k_D = 2$ and $k_I = 10$.

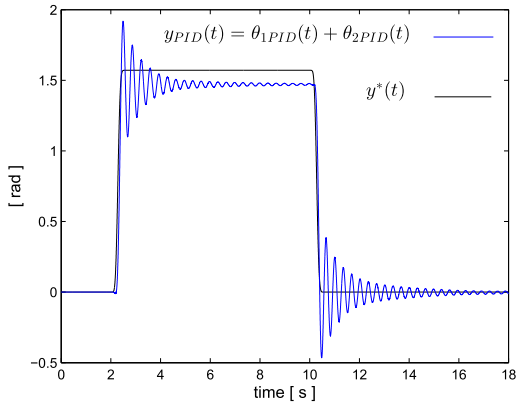


FIGURE 4. Flexible-Joint Robot Arm performance with PID controller.

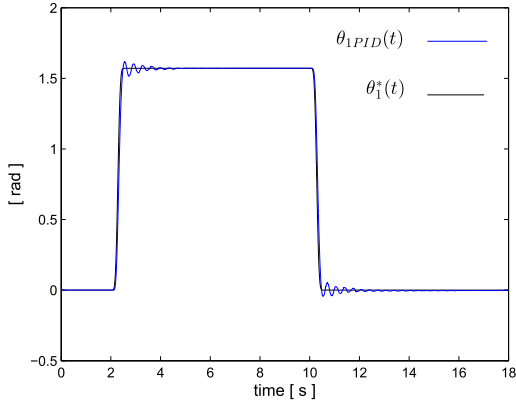


FIGURE 5. The rotating base trajectory tracking.

Figure 4 shows the Flexible-Joint Robot Arm experimental platform performance. While, the rotating base follows the desired trajectory $y^*(t)$ (see, Figure 5), the link tip presents undesirable oscillations when the rotating base accomplish the rest positions, which occurs at $t = 2.6[\text{s}]$ and $t = 10.6[\text{s}]$. In Figure 6, the tracking error $e_{yPID}(t) = y_{PID}(t) - y^*(t)$ is depicted. As we can see, the maximum amplitude of $e_{yPID}(t)$ is approximately $0.6[\text{rad}]$ and it decrease exponentially with a frequency of oscillation $f = 2.75[\text{Hz}]$. The effects of the gravity affecting the system can be clearly appreciated when the rotating base arrive to reference $y^*(2.6) = \frac{\pi}{2}[\text{rad}]$, as a consequence of this effects, an offset of $0.1[\text{rad}]$ appears on the position of the link tip with respect to the tracking reference.

The control voltage applied to the motor $V_{PID}(t)$ is depicted in Figure 7. Here, we can notice that when the oscillations

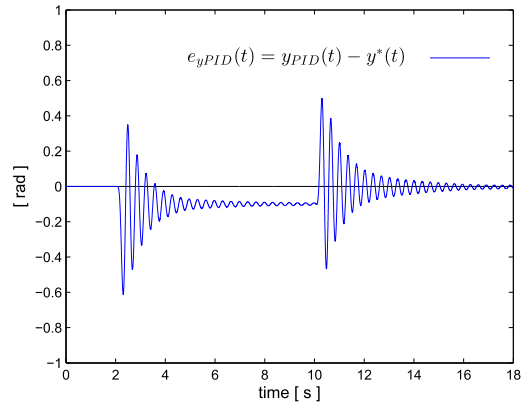


FIGURE 6. Output reference trajectory tracking error evolution.

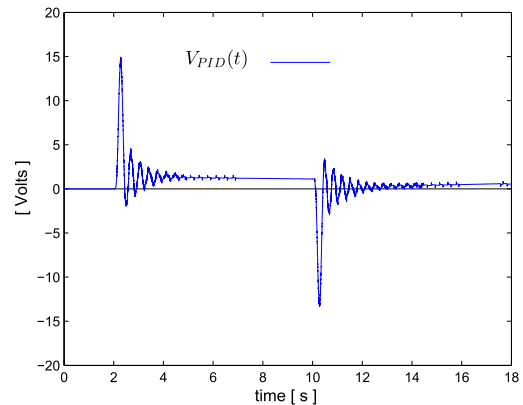


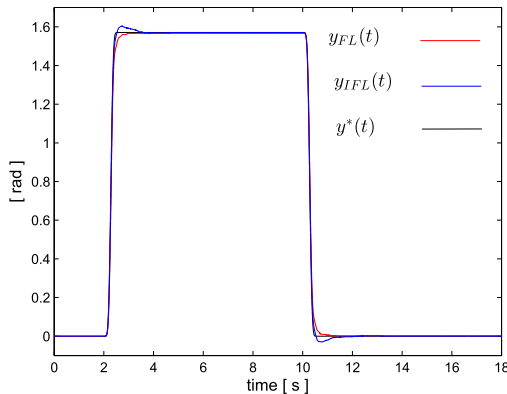
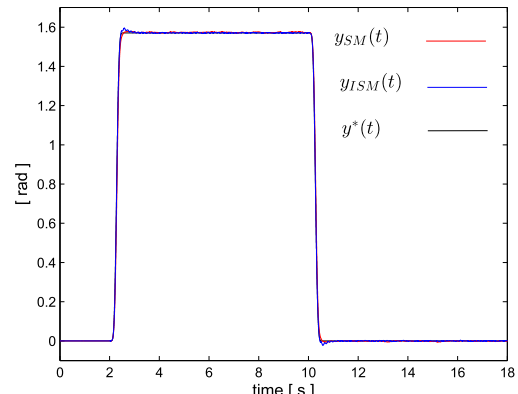
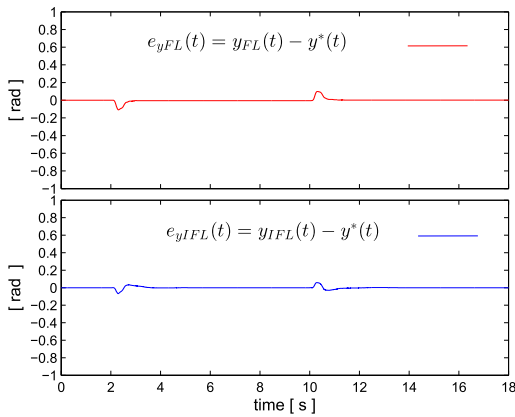
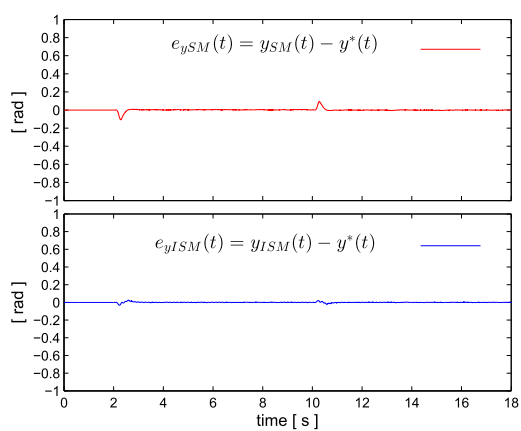
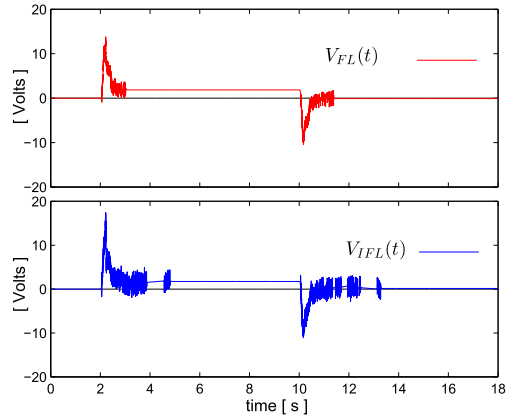
FIGURE 7. Control input voltage for output reference trajectory tracking task.

occur, they affect the angular position of the base $\theta_{1PID}(t)$, and as it was shown in Figure 5, the controller tries to compensate the dynamics produced by the oscillations.

3) FEEDBACK LINEARIZATION CONTROLLER

The oscillations due to the flexibility of the system, makes it difficult to control the position of end-point in an effective manner. In order to achieve the suppression of oscillations, we use an exact feedback linearization controller (FL), of the form (7) and a integral feedback linearization controller (IFL), developed in Section III-A. The FL controller design parameters (9) were specified using the values $\xi_{FL} = 1.4$, $\omega_{FL} = 45$, and IFL controller parameters were choose as $\xi_{IFL} = 2.5$, $\omega_{IFL} = 30$ and $p_{IFL} = 20$. The output is defined as the angular position of end-point of arm, that is $y_{FL}(t)$ and $y_{IFL}(t)$ for both controllers are shown in Figure 8. It becomes evident the suitable tracking quality of the schemes, the arm's end-point position carry out the trajectory tracking task without oscillations.

The tracking error e_{yFL} and e_{yIFL} of the system are shown in Figure 9, where can observe, that the position error is restricted to a small vicinity and it is seen to be uniformly bounded, in the steady state, and it is smaller in comparison to e_{yPID} (see, Figure 6). The control voltage $V_{FL}(t)$ and $V_{IFL}(t)$

**FIGURE 8.** End-point position performance of the FL and IFL controllers.**FIGURE 11.** End-point position performance of the SM and ISM controllers.**FIGURE 9.** Output reference trajectory tracking error (Feedback linearization).**FIGURE 12.** Output reference trajectory tracking error (Sliding Mode controller).**FIGURE 10.** Control input voltage (Feedback linearization).

is depicted in Figure 10. In contrast of the PID control voltage, here the peak voltage is smaller and cancel out the undesirable oscillations.

4) SUPER-TWISTING SLIDING MODE CONTROLLER

In order to test the performance of the feedback linearization scheme, we carried out a comparative analysis with respect to a super twisting sliding mode controller (SM) and integral

super twisting sliding mode controller (ISM) that is a well-known robust control scheme. Taking advantage of feedback linearization, the implementation of a sliding mode based control scheme is feasible, see [32]. The design parameters (11) of the SM controller were chosen according the values $\xi_{SM} = 1.4$, $\omega_{SM} = 25$ and $p_{SM} = 20$, $W = 2789600$, $a = 7000$, $\delta = 100$. The parameters for ISM (15) were set using the following values $\xi_{ISM} = 1.5$, $\omega_{SM} = 20$ and $W = 2789600$, $a = 7000$, $\delta = 100$. The output is specified as the angular position of end-point of arm as $y_{SM}(t)$ and $y_{ISM}(t)$ are shown in Figure 11. We can notice the acceptable performance in the tracking trajectory task, avoiding oscillations and reducing the tracking error when the link tip arrive to the rest positions in comparison with y_{FL} and y_{IFL} tracking trajectory. The tracking error $e_{ySM}(t)$ and $e_{yISM}(t)$ are detailed in Figure 12. It is restricted to a vicinity of radius 0.1 [rad] approximately, and in comparison of the error in the Feedback linearization scheme $e_{yFL}(t)$ and $e_{yIFL}(t)$, are significantly smaller. The control voltages $V_{SLM}(t)$ and $V_{ISM}(t)$ are provided in Figure 13 which tend to cancel out the additive endogenous disturbance inputs produced by dynamic of the system, defined in (13), and the controllers show a minimal chattering during all the operation. Chattering is undesirable

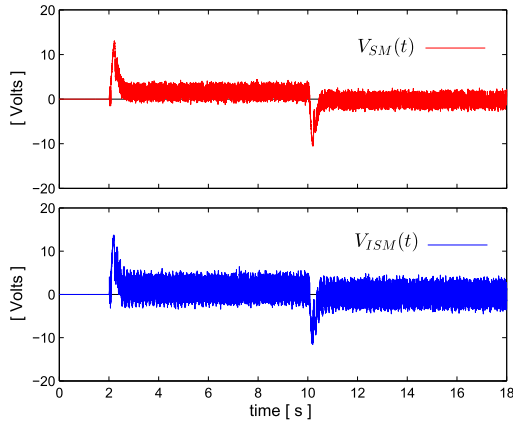


FIGURE 13. Control input voltage (Sliding Mode controller).

behavior could damage the motor, amplifiers or even the pulley-belt system. A Quadratic Error Index of the form:

$$ISI(t) = \int_0^t [y(\tau) - y^*(\tau)]^2 d\tau \quad (20)$$

is used to compare the performances obtained, with FL and SM controllers tested, Figure 14 shows that ISM control leads to a minimal performance index $ISI_{ISM}(t)$ in contrast to the results obtained with the $ISI_{ISM}(t)$, $ISI_{FL}(t)$ and $ISI_{IFL}(t)$ based controllers.

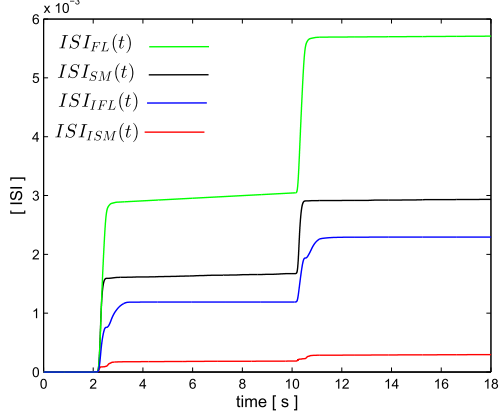


FIGURE 14. Performance index of the implemented controllers.

C. EXTERNAL PERTURBATION TEST

The controllers proposed have a good performance using a total knowledge of dynamic model of the flexible robot link, In order to test the controller robustness in presence of an external un-modeled perturbation, we add arm a pendulum actuated by a RC servomotor as show Figure 15, pendulum length is $l_p = 0.20[m]$ with a mass on the top of $m_p = 0.050[Kg]$, the RC servomotor mass is $m_s = 0.050[Kg]$. The initial condition of pendulum is $0[\text{rad}]$, it place mass m_p at $0.05[m]$ from pivot arm, when time is $t = 3[s]$ after the reference trajectory arrive $y^*(3) = \frac{\pi}{2}$ the pendulum is moved to $\pi[\text{rad}]$ in a $1[s]$ placed the

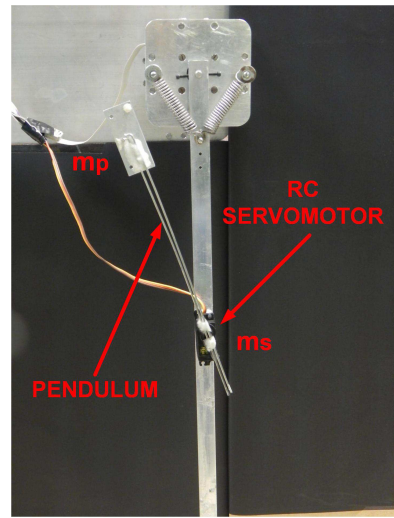


FIGURE 15. External perturbation pendulum.

mass m_p at $0.45[m]$ from pivot arm and remains in this position for 4 seconds, when the time is $t = 8[s]$ the pendulum returns to initial condition, we use the same gains computed for unperturbed test.

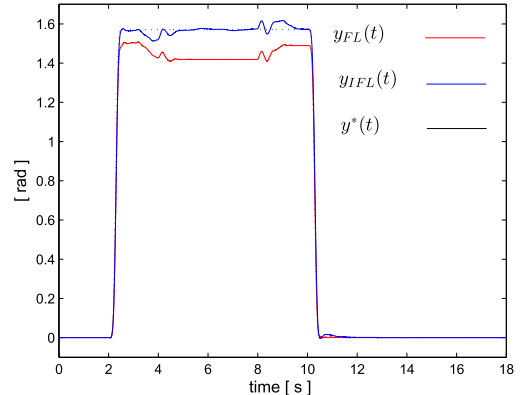


FIGURE 16. End-point position performance (Feedback linearization).

The perturbed angular position end-point arm using feedback linearization schemes are shown in Figure 16, $y_{FL}(t)$ tracking trajectory avoid oscillations but show steady state error due to un modeled mass m_p and m_s added, when the pendulum change of position tracking trajectory steady state error increase as a consequence of the arm center of mass is changed, in the other hand integral feedback linearization output $y_{IFL}(t)$ eliminate steady state error with overshoot when the pendulum is moved at time is $t = 3[s]$ and $t = 8[s]$. Figure 17 depicts the tracking trajectory error e_{yFL} and e_{yIFL} , we can notice that the IFL has a good performance in spite of external perturbation respect of FL , the control input V_{IFL} has a major amplitude compared with V_{FL} , see Figure 18.

The perturbed angular position end-point arm using second order slide mode control schemes are shown in Figure 19, $y_{SM}(t)$ has the same performance compared with $y_{FL}(t)$

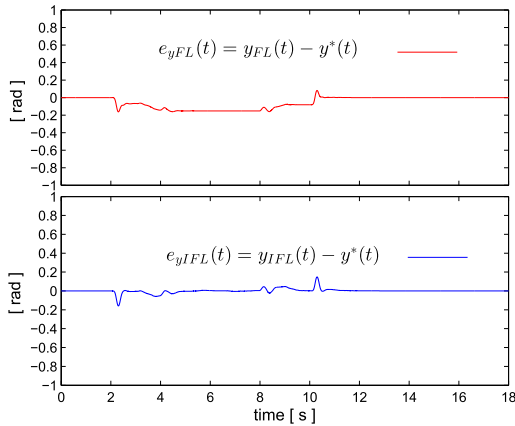


FIGURE 17. Output reference trajectory tracking error (Feedback linearization).

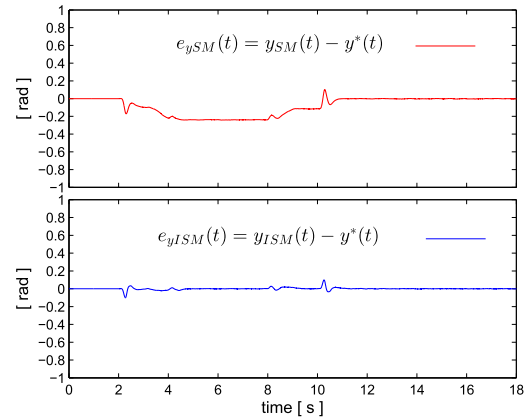


FIGURE 20. Output reference trajectory tracking error (Sliding Mode controller).

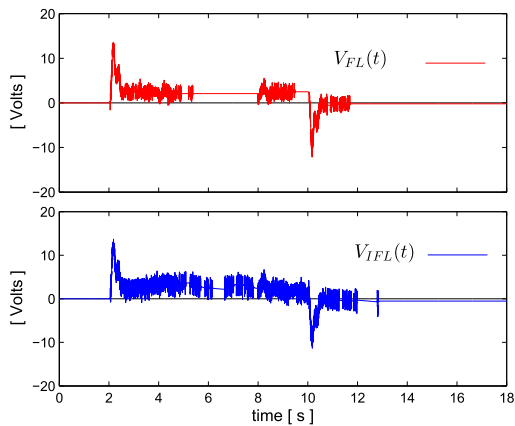


FIGURE 18. Control input voltage (Feedback linearization).

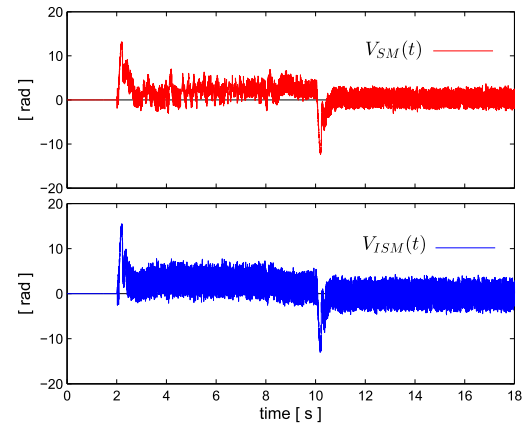


FIGURE 21. Control input voltage (Sliding Mode controller).

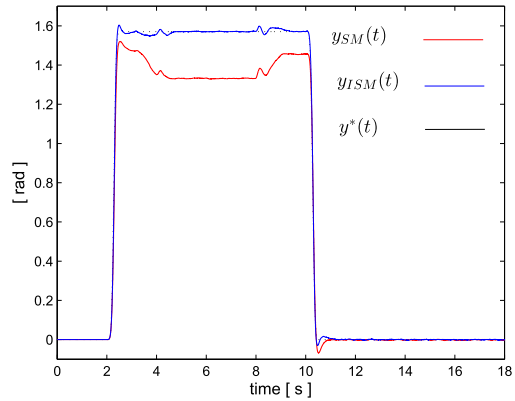


FIGURE 19. End-point position performance (Sliding Mode controller).

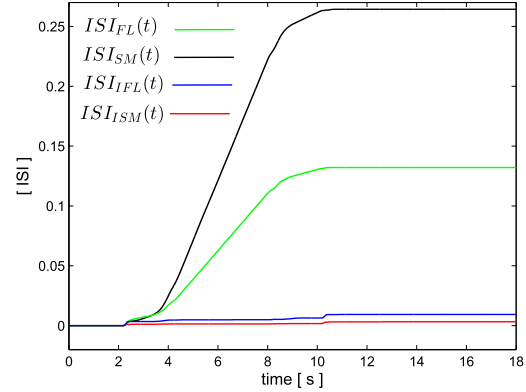


FIGURE 22. Performance index of the implemented controllers, in presence of external un-modeled perturbations.

presented in Figure 16, external perturbation produce a tracking trajectory steady state error, but integral second order slide mode control $y_{ISM}(t)$ eliminate steady state error with better performance than $y_{IFL}(t)$ even when pendulum is moved at time $t = 3[s]$ and $t = 8[s]$ as show the tracking trajectory error e_{yISM} depicted in Figure 20. ISM has the smallest error, the control input signal V_{ISM} , depicted

in Figure 21, cancels out the external perturbation with the minimal error. Integral Feedback linearization and Integral second order slide mode control avoid oscillations and are robust in a presence of external un-modeled perturbations. It can be also observed in Figure 22 where a minimal performance index is achieved by $ISI_{ISM}(t)$ and $ISI_{IFL}(t)$, compared with the results obtained with the $ISI_{FL}(t)$, and $ISI_{IS}(t)$ based controllers.

V. CONCLUSIONS

In this work, the tracking control problem of flexible joint robot was addressed. Two control laws are proposed for the task of trajectory tracking. Two nonlinear control schemes, one model based and another one of discontinuous class were selected to increase the performance of the classic schemes, with the aim of avoiding oscillations on the robot arm tip. State space dynamics description of flexible joint is used in order to design the nonlinear control schemes. By dynamic feedback linearization methodology, the robot dynamics was modified into a linear and controllable chain of integrators, to be then controlled by a full state feedback control. In order to reject nonlinearities in the state space description, while avoiding oscillation effect in the flexible joint robot arm, a sliding mode control was proposed. The experimental results show that the proposed nonlinear control laws, feedback linearization and slide mode control, are efficient in achieving precise moving of the robot if the dynamic model is exactly known, but the performance of both controllers decrease when unmodeled dynamics and disturbance are applied to the system. To increase the robustness we implemented an integral compensator for feedback linearization controller, in the same way we introduce a integral compensator in the sliding manifold. The experimental results show more efficient result with bounded error, where slide mode control has the best performance. An extension of the problem may consist in the use of schemes based in compensator networks. Another suggestion for further study consists in the use of Generalized Proportional Integral Control.

ACKNOWLEDGMENT

This work was partially supported by SIP-IPN under the research grant SIP-20160354 and Secretaría de Ciencia, Tecnología e Innovación de la Ciudad de México (Project SECITI 2016-272).

REFERENCES

- [1] G. Bartolini, A. Ferrara, and E. Usai, "Chattering avoidance by second-order sliding mode control," *IEEE Trans. Autom. Control*, vol. 43, no. 2, pp. 241–246, Feb. 1998.
- [2] G. Bartolini, A. Pisano, and E. Usai, "Second-order sliding-mode control of container cranes," *Automatica*, vol. 38, no. 10, pp. 1783–1790, Oct. 2002.
- [3] M. M. Bridges, D. M. Dawson, and C. T. Abdallah, "Control of rigid-link, flexible-joint robots: A survey of backstepping approaches," *J. Field Robot.*, vol. 12, no. 3, pp. 199–216, Mar. 1995.
- [4] R. J. Caverly, D. E. Zlotnik, L. J. Bridgeman, and J. R. Forbes, "Saturated proportional derivative control of flexible-joint manipulators," *Robot. Comput.-Integr. Manuf.*, vol. 30, no. 6, pp. 658–666, Dec. 2014.
- [5] A. Chalanga, S. Kamal, L. Fridman, B. Bandyopadhyay, and J. A. Moreno, "How to implement super-twisting controller based on sliding mode observer?" in *Proc. IEEE 13th Int. Workshop Variable Struct. Syst. (VSS)*, Jun. 2014, pp. 1–6.
- [6] S.-B. Choi, C.-C. Cheong, and H.-C. Shin, "Sliding mode control of vibration in a single-link flexible arm with parameter variations," *J. Sound Vibrat.*, vol. 179, no. 5, pp. 737–748, Feb. 1995.
- [7] A. De Luca, A. Isidori, and F. Nicolo, "Control of robot arm with elastic joints via nonlinear dynamic feedback," in *Proc. 24th IEEE Conf. Decision Control*, Dec. 1985, pp. 1671–1679.
- [8] A. De Luca and L. Lanari, "Robots with elastic joints are linearizable via dynamic feedback," in *Proc. 34th IEEE Conf. Decision Control*, vol. 4, Dec. 1995, pp. 3895–3897.
- [9] M. M. Fateh, "Nonlinear control of electrical flexible-joint robots," *Nonlinear Dyn.*, vol. 67, no. 4, pp. 2549–2559, Mar. 2012.
- [10] M. M. Fateh, "Robust control of flexible-joint robots using voltage control strategy," *Nonlinear Dyn.*, vol. 67, no. 2, pp. 1525–1537, Jan. 2012.
- [11] E. Gurkan, S. P. Banks, and I. Erkmen, "Stable controller design for the T-S fuzzy model of a flexible-joint robot arm based on Lie algebra," in *Proc. 42nd IEEE Conf. Decision Control*, vol. 5, Dec. 2003, pp. 4714–4722.
- [12] D. Hrovat, P. Barak, and M. Rabins, "Semi-active versus passive or active tuned mass dampers for structural control," *J. Eng. Mech.*, vol. 109, no. 3, pp. 691–705, Aug. 1983.
- [13] H.-P. Huang and W.-M. Lin, "Control of a flexible robot arm using simplified fuzzy controllers," *Int. J. Fuzzy Syst.*, vol. 2, no. 1, pp. 67–77, 2000.
- [14] Š. Ileš, A. Ivančić, J. Matuško, and F. Kolonić, "Mechatronic design and control of rotary flexible joint," in *Proc. 15th Int. Power Electron. Motion Control Conf. (EPE/PEMC)*, Sep. 2012, pp. DS3d.9-1–DS3d.9-6.
- [15] A. Isidori, *Nonlinear control systems*. Springer: Berlin, 1995.
- [16] M. Khairudin, Z. Mohamed, and A. R. Husain, "Dynamic model and robust control of flexible link robot manipulator," *TELKOMNIKA (Telecommun. Comput. Electron. Control.)*, vol. 9, no. 2, pp. 279–286, 2013.
- [17] S. Kurode and P. Dixit, "Control of tip position of flexible link manipulator using sliding modes," *System*, vol. 3, p. 5, 2012.
- [18] H. Lee, Y. Oh, and J.-B. Song, "Torque sensor based robot arm control using disturbance observer," in *Proc. Int. Conf. Control Autom. Syst. (ICCAS)*, Oct. 2010, pp. 1697–1700.
- [19] L. E. Lester et al., "Range of motion of the metacarpophalangeal joint in rheumatoid patients, with and without a flexible joint replacement prosthesis, compared with normal subjects," *Clin. Biomech.*, vol. 27, no. 5, pp. 449–452, Jun. 2012.
- [20] A. Levant, "Higher-order sliding modes, differentiation and output-feedback control," *Int. J. Control.*, vol. 76, nos. 9–10, pp. 924–941, 2003.
- [21] R. Lozano and B. Brogliato, "Adaptive control of robot manipulators with flexible joints," *IEEE Trans. Autom. Control*, vol. 37, no. 2, pp. 174–181, Feb. 1992.
- [22] H. A. Malki, D. Misir, D. Feigenspan, and G. Chen, "Fuzzy PID control of a flexible-joint robot arm with uncertainties from time-varying loads," *IEEE Trans. Control Syst. Technol.*, vol. 5, no. 3, pp. 371–378, May 1997.
- [23] M. Mirshekaran, F. Piltan, Z. Esmaeili, T. Khajehian, and M. Kazeminasab, "Design sliding mode modified fuzzy linear controller with application to flexible robot manipulator," *Int. J. Modern Educ. Comput. Sci. (IJMECS)*, vol. 5, no. 10, pp. 53–63, Nov. 2013.
- [24] Z. Mohamed and M. O. Tokhi, "Command shaping techniques for vibration control of a flexible robot manipulator," *Mechatronics*, vol. 14, no. 1, pp. 69–90, Feb. 2004.
- [25] J. A. Moreno and M. Osorio, "Strict Lyapunov functions for the super-twisting algorithm," *IEEE Trans. Autom. Control*, vol. 57, no. 4, pp. 1035–1040, Apr. 2012.
- [26] A. Mujumdar, S. Kurode, and B. Tamhane, "Fractional order sliding mode control for single link flexible manipulator," in *Proc. IEEE Int. Conf. Control Appl. (CCA)*, Aug. 2013, pp. 288–293.
- [27] S. Ozgoli and H. D. Taghirad, "A survey on the control of flexible joint robots," *Asian J. Control*, vol. 8, no. 4, pp. 332–344, Dec. 2006.
- [28] H. W. Park, H. S. Yang, Y. P. Park, and S. H. Kim, "Position and vibration control of a flexible robot manipulator using hybrid controller," *Robot. Auto. Syst.*, vol. 28, no. 1, pp. 31–41, Jul. 1999.
- [29] H. Rodríguez, A. Astolfi, and R. Ortega, "On the construction of static stabilizers and static output trackers for dynamically linearizable systems, related results and applications," *Int. J. Control.*, vol. 79, no. 12, pp. 1523–1537, 2006.
- [30] A. Sanz and V. Etxebarria, *Experimental Control of Flexible Robot Manipulators*. Rijeka, Croatia: InTech, 2008.
- [31] Y. Shtessel, C. Edwards, L. Fridman, and A. Levant, *Sliding mode control and observation*. Springer: New York, 2014.
- [32] H. Sira-Ramírez, "On the sliding mode control of nonlinear systems," *Syst. control Lett.*, vol. 19, no. 4, pp. 303–312, 1992.
- [33] J. F. P. Solís, G. S. Navarro, and R. C. Linares, "Modeling and tip position control of a flexible link robot: Experimental results," *Comput. Sistemas*, vol. 12, no. 4, pp. 421–435, 2009.
- [34] M. W. Spong, "Modeling and control of elastic joint robots," *J. Dyn. Syst., Meas., Control*, vol. 109, no. 4, pp. 310–318, Dec. 1987.
- [35] M. W. Spong, "Adaptive control of flexible joint manipulators: Comments on two papers," *Automatica*, vol. 31, no. 4, pp. 585–590, Apr. 1995.

- [36] B. Subudhi and A. S. Morris, "Soft computing methods applied to the control of a flexible robot manipulator," *J. Appl. Soft Comput.*, vol. 9, no. 1, pp. 149–158, Jan. 2009.
- [37] S. E. Talole, J. P. Kolhe, and S. B. Phadke, "Extended-state-observer-based control of flexible-joint system with experimental validation," *IEEE Trans. Ind. Electron.*, vol. 57, no. 4, pp. 1411–1419, Apr. 2010.
- [38] W. Tang and G. Chen, "A robust fuzzy pi controller for a flexible-joint robot arm with uncertainties," in *Proc. 3rd IEEE Conf. Fuzzy Syst., IEEE World Congr. Comput. Intell.*, Jun. 1994, pp. 1554–1559.
- [39] P. Tomei, "A simple PD controller for robots with elastic joints," *IEEE Trans. Autom. Control*, vol. 36, no. 10, pp. 1208–1213, Oct. 1991.
- [40] V. Utkin, J. Guldner, and J. Shi, *Sliding Mode Control in Electro-Mechanical Systems*, vol. 34. Boca Raton, FL, USA: CRC Press, 2009.
- [41] C. Vázquez, J. Collado, and L. Fridman, "Super twisting control of a parametrically excited overhead crane," *J. Franklin Inst.*, vol. 351, no. 4, pp. 2283–2298, Apr. 2014.
- [42] L. Villani and J. De Schutter, "Force control," in *Springer handbook of robotics*. Springer: Berlin, 2008, pp. 161–185.
- [43] G. A. Wilson and G. W. Irwin, "Robust tracking of elastic joint manipulators using sliding mode control," *Trans. Inst. Meas. Control*, vol. 16, no. 2, pp. 99–107, Apr. 1994.
- [44] S. Wolf and G. Hirzinger, "A new variable stiffness design: Matching requirements of the next robot generation," in *Proc. IEEE Int. Conf. Robot. Autom. (ICRA)*, May 2008, pp. 1741–1746.
- [45] L. Zouari, H. Abid, and M. Abid, "Flexible joint manipulator based on backstepping controller," in *Proc. 15th Int. Conf. Sci. Techn. Autom. Control Comput. Eng. (STA)*, Dec. 2014, pp. 330–334.
- [46] E. W. Zurita-Bustamante, J. Linares-Flores, E. Guzman-Ramirez, and H. Sira-Ramirez, "A comparison between the GPI and PID controllers for the stabilization of a DC–DC 'Buck' converter: A field programmable gate array implementation," *IEEE Trans. Ind. Electron.*, vol. 58, no. 11, pp. 5251–5262, Nov. 2011.



MARIO RAMÍREZ-NERIA received the B.S. degree in mechatronics engineering from UPIITA and the M.S. degree in electrical engineering from CINVESTAV, Electrical Engineering Department, Mechatronics Section, National Polytechnic Institute (IPN), Mexico City, Mexico. He is currently pursuing the Ph.D. degree with CINVESTAV, Automatic Control Department, IPN. His current research interests are applications of control theory, active disturbance rejection control, mechanical underactuated system, and robotics.



GILBERTO OCHOA-ORTEGA was born in Mexico City, Mexico, in 1979. He received the degree from the National Polytechnic Institute, Mexico, in 2003, and the master's and Ph.D. degrees from CINVESTAV, Automatic Control Department, in 2006 and 2010, respectively. Since 2009, he has been with the Division of Mechatronics, Mexico's Valley Polytechnic University. His research interests include time delay systems, linear systems, and control of mechatronics systems.



NORMA LOZADA-CASTILLO received the degree from the Superior School of Physics and Mathematics, and the master's and Ph.D. degrees from CINVESTAV, Automatic Control Department, National Polytechnic Institute. Her research interests include stochastic control, nonlinear control, and estimation in stochastic systems.



MIGUEL ANGEL TRUJANO-CABRERA was born in Mexico City, in 1982. He received the B.S. degree in mechatronics engineering from the National Polytechnic Institute in 2005, and the M.Sc. and Ph.D. degrees in automatic control from CINVESTAV, Department of Automatic Control, in 2008 and 2012, respectively. Since 2013, he has been with the Division of Mechatronics, Mexico's Valley Polytechnic University. His research interests include robotics, artificial vision, and mechatronic systems.



JUAN PABLO CAMPOS-LOPEZ was born in Mexico City, Mexico, in 1982. He received the B.S. degree in mechanic engineering from the UNAM in 2005, and the M.Sc. and Ph.D. degrees in mechanical engineering from the National Polytechnic Institute, in 2008 and 2012, respectively. Since 2012, he has been with the Division of Mechatronics, Mexico's Valley Polytechnic University. His research interests include mechatronics systems, and strain measurements with



ALBERTO LUVIANO-JUÁREZ was born in Mexico City, Mexico, in 1981. He received the B.S. degree in mechatronics engineering from the National Polytechnic Institute (IPN), Mexico, in 2003, the M.Sc. degree in automatic control from CINVESTAV, Automatic Control Department, IPN, in 2006, and the Ph.D. degree in electrical engineering from CINVESTAV, Department of Electrical Engineering, Mechatronics Section, in 2011. Since 2011, he has been with the Postgraduate and Research Section, UPIITA, IPN. His research interests include robust estimation and control in mechatronic systems, robotics, and algebraic methods in the estimation and control of mechatronic systems.